# Design of a Novel Class of Peptide Inhibitors of Cyclin-dependent Kinase/Cyclin Activation

Claire Gondeau, Sabine Gerbal-Chaloin, Paul Bello, Gudrun Aldrian-Herrada, May Morris, Gilles Divita

THE JOURNAL OF BIOLOGICAL CHEMISTRY
Vol. 280, No. 14, Issue of April 8, pp. 13793–13800, 2005
Printed in U.S.A.


# Design of a Novel Class of Peptide Inhibitors of Cyclin-dependent Kinase/Cyclin Activation*

Received for publication, December 6, 2004, and in revised form, January 11, 2005
Published, JBC Papers in Press, January 13, 2005, DOI 10.1074/jbc.M413690200

**Claire Gondeau‡§, Sabine Gerbal-Chaloin‡¶, Paul Bello‖, Gudrun Aldrian-Herrada‡, May C. Morris‡, and Gilles Divita‡****

*From the ‡Centre de Recherches de Biochimie Macromoléculaire, Department of Molecular Biophysics and Therapeutics, FRE-2593 CNRS, 1919 Route de Mende, 34293 Montpellier, France and ‖Stem Cell Sciences Limited, P. O. Box 8224, Monash University L. P. O., Clayton, Victoria 3168, Australia*

**Cyclin dependent kinases (CDKs) are key regulators of the cell cycle progression and therefore constitute excellent targets for the design of anticancer agents. Most of the inhibitors identified to date inhibit kinase activity by interfering with the ATP-binding site of CDKs. We recently proposed that the protein/protein interface and conformational changes required in the molecular mechanism of CDK2-cyclin A activation were potential targets for the design of specific inhibitors of cell cycle progression. To this aim, we have designed and characterized a small peptide, termed C4, derived from amino acids 285–306 in the α5 helix of cyclin A. We demonstrate that this peptide does not interfere with complex formation but forms stable complexes with CDK2-cyclin A. The C4 peptide significantly inhibits kinase activity of complexes harboring CDK2 in a competitive fashion with respect to substrates but does not behave as an ATP antagonist. Moreover, when coupled with the protein transduction domain of Tat, the C4 peptide blocks the proliferation of tumor cell lines, thereby constituting a potent lead for the development of specific CDK-cyclin inhibitors.**

In higher eukaryotes, cell cycle progression is coordinated by several closely related Ser/Thr protein kinases resulting from the association of a catalytic cyclin-dependent kinase (CDK)[1] subunit with a regulatory cyclin subunit (1). CDK-cyclin complexes are regulated by both phosphorylation/dephosphorylation and protein-protein interactions with different partners, including structural CDK inhibitors. Genetic evidence supports a strong correlation between alterations in the regulation of CDKs and the molecular pathology of cancer (2). Thus, in the past few years there has been considerable interest in the development of inhibitors of CDK protein kinases (3–5). A greater understanding of the cell cycle and the inherent complexity of CDK regulation offer a number of possible routes to its inhibition (6). One of the currently most developed strategies to inhibit CDKs is based on the design of small molecules that target the ATP-binding site, thereby interfering directly with their catalytic activity. Despite the high degree of sequence conservation between the catalytic clefts of protein kinase family members, a number of kinase-specific ATP antagonists have been characterized (7–10). Another strategy for blocking malignant cellular proliferation involves the design of peptide-based inhibitors that target the substrate recruitment binding groove identified on cyclin partners and on a number of cell cycle regulatory proteins (11). Recognition of this groove is mediated by a specific sequence termed the cyclin binding motif (CBM). Several CBM-derived peptides have been reported to induce either cell cycle arrest or apoptosis in tumor cells *in vitro* (12, 13) and *in vivo* (14) when conjugated to cellular delivery vectors.

Determination of the crystal structure of several CDK and CDK-cyclin complexes has provided essential information on the mechanism of formation and activation of these protein kinases (15). Upon binding to CDK2, cyclin A induces a marked structural reorganization of the catalytic kinase subunit (16), which involves rearrangement of the PSTAIRE helix and repositioning of the relative orientation of the N- and C-terminal lobes. The α3 and α5 helices of cyclin A clamp the PSTAIRE at its center through hydrogen bonds, thereby promoting reconfiguration of the ATP-binding site. The cyclin also interacts with the T-loop of CDK2, causing this loop to move away from the active site. A fully active complex is finally generated through the phosphorylation of CDK2 on $Thr^{160}$, which induces further changes in the orientation of the T-loop and promotes additional contacts with cyclin A. In contrast, comparison of the crystal structures of cyclin A in its free (17) and CDK2-bound state (16) indicates that this regulatory subunit does not undergo any conformational changes upon complex formation.

We have recently demonstrated that the molecular mechanism of CDK2-cyclin A complex formation is a two-step process (18). The first step involves the rapid association between the PSTAIRE helix of CDK2 and helices α3 and α5 of the cyclin to yield a non-processive intermediate complex. Two residues in the PSTAIRE helix, $Ile^{49}$ and $Arg^{50}$, located in a hydrophobic pocket in close contact with the side chains of $Lys^{263}$, $Lys^{266}$, and $Phe^{267}$ and those of $Leu^{299}$ and $Leu^{306}$ within the α3 and α5 helices of cyclin A, respectively, are essential for the initial assembly of the CDK-cyclin complex. The second step involves additional contacts between the C-lobe of the CDK and the N-terminal helix of the cyclin, which induce subsequent isomerization of the CDK into a fully mature form by promoting exposure of the T-loop for phosphorylation by the CDK-activating kinase (CAK) as well as formation of the substrate-binding site. Both the conformational changes of the non-processive intermediate and phosphorylation have been reported to control the selectivity of the CDK for its cyclin

* This work was supported in part by CNRS and grants from the French Association pour la Recherche contre le Cancer Grants ARC-4326 (to M. C. M.) and ARC-5271 (to G. D.). The costs of publication of this article were defrayed in part by the payment of page charges. This article must therefore be hereby marked "*advertisement*" in accordance with 18 U.S.C. Section 1734 solely to indicate this fact.
§ Supported by a grants from HMR-Aventis, Sidaction.
¶ Supported by European Commission Grant QLK2-CT-2001-01451.
** To whom correspondence should be addressed. Tel.: 33-04-6761-3392; Fax: 33-04-6752-1559; E-mail: gilles.divita@crbm.cnrs.fr.
[1] The abbreviations used are: CDK, cyclin-dependent kinase; CBM, cyclin binding motif; CD, circular dichroism; Fmoc, *N*-(9-fluorenyl)methoxycarbonyl; GST, glutathione *S*-transferase; Rb, retinoblastoma.

partner (19, 20). We suggest that the steps of assembly and the activation of CDK-cyclin complexes both constitute key targets for the development of specific inhibitors.

In the present work, we propose a new strategy to selectively inhibit kinase activity of CDK-cyclin complexes by targeting the protein/protein interface between the two subunits. We have designed a peptide of 22 residues derived from the α5 helix of cyclin A that forms stable complexes with CDK2-cyclin A. We demonstrate that this peptide inhibits CDK2 kinase activity in a competitive fashion with respect to protein substrates. Moreover, when coupled to the protein transduction domain of Tat, this peptide blocks proliferation of tumor cell lines and therefore constitutes a potent lead for the development of specific CDK-cyclin inhibitors.

## EXPERIMENTAL PROCEDURES

*Chemicals—N,N*-Dimethylformamide, piperidine, trifluoroacetic acid, and $CH_3CN$ (high performance liquid chromatography grade) were purchased from SDS (Peypin, France). The protected amino acids were from SENN Chemicals (Dielsdorf, Switzerland). *O*-Hexafluorophospho-[7-azabenzotriazol-1-yl]-*N*,*N*,*N*′,*N*′-tetramethyluronium (HATU), diisopropylethylamine (DIEA), and resins were from Applied Biosystems (Foster City, CA), and thioanisole, ethanedithiol, and triisopropylsilane were from Sigma-Aldrich.

*Peptide Synthesis and Purification*—All peptides were synthesized using an Fmoc continuous flow apparatus (Pioneer™; Applied Biosystems) starting from Fmoc-peptide amide liner-polyethylene glycol-polystyrene resins at a 0.2-mmol scale. The coupling reactions were performed with 0.5 M HATU in the presence of 1 M DIEA. Protecting group removal and final cleavage from the resin were carried out with trifluoroacetic acid/phenol/$H_2O$/thioanisol/ethanedithiol (82.5:5:5:5:2.5%) for 4 h and 20 min for peptides C1, C3, and C7 and with trifluoroacetic acid/phenol/$H_2O$/triisopropylsilane (88:5:5:2%) for 4 h in the case of C5, C4, and C8. Crude peptides were purified by semi-preparative reverse phase high performance liquid chromatography on a C18 column (Interchrom UP5 WOD/25 M Uptisphere 300, 5 ODB, 250 × 21.2 mm) and identified by electrospray mass spectrometry. Tat, C2, C6, and C9 peptides were obtained from NeoMPS (Strasbourg-France). The C4 peptide was conjugated to the Tat peptide GRKKRRQRRR-C through a disulfide bond using the cysteamide function at the C terminus of C4. All peptides were dissolved with deionized water to make a stock solution of 500 μM except for C1 and C8 which, because of their poor solubility in water, were first dissolved in dimethyl sulfoxide. Peptides were then diluted in phosphate-buffered saline (8.1 mM $Na_2HPO_4$, 1.47 mM $KH_2PO_4$, 2.67 mM KCl, and 138 mM NaCl).

*Protein Expression and Purification*—The GST-retinoblastoma fusion protein (GST-Rb), harboring residues 792 to 928, was provided by C. Sardet (IGMM, Montpellier, France). CDK2-cyclin E and CDK1-cyclin B1 complexes were purified from baculovirus-infected insect cell lysates as described previously (21, 22). Human CDK2 phosphorylated on $Thr^{160}$ was produced in *Escherichia coli* (BL21) by coexpression of GST-CDK2 and *Saccharomyces cerevisiae* GST-CIV1 (a gift from J. Endicott, Laboratory of Molecular Biophysics and Oxford Centre for Molecular Sciences, Oxford, UK). Full-length human cyclin A was expressed as an untagged or a GST-tagged protein in *E. coli.* Monomeric proteins as well as the CDK2-cyclin A complex were purified according to Brown *et al.* (17). Briefly, cells expressing GST-CDK2 or cyclin A were lysed by sonication on ice. The clarified lysate of GST-CDK2 was applied onto a glutathione-Sepharose column (Amersham Biosciences) equilibrated in buffer A (40 mM HEPES, pH 7.0, 200 mM NaCl, and 0.01% (v/v) monothioglycerol) and extensively washed. The clarified lysate of cyclin A was then applied onto the CDK2-bound glutathione-Sepharose column. The GST-CDK2-cyclin A complex was eluted with buffer A containing 20 mM glutathione (Sigma). Following cleavage of the GST tag with protease 3C (1:50) (w/w) at 4 °C for 12 h, CDK2-cyclin A was purified by size exclusion chromatography on a HiLoad 16/60 Superdex 75 column (Amersham Biosciences). Fractions containing CDK2-cyclin A were pooled and further purified by exclusion from glutathione-Sepharose.

*Kinase Assays*—CDK kinase assays were carried out in a final volume of 30 μl containing 3 μM histone H1 (H4524; Sigma) or GST-Rb or 0.4 mM peptide substrate (histone H1-derived peptide PKTPKKAKKL; Promega Corporation, Madison, WI), 50 μM cold ATP, and 0.15 μCi [γ-$^{32}$P]ATP (3000 Ci/mmol; Amersham Biosciences). The kinase concentration used was 20 nM. Reactions were performed for 15 min at 25 °C and then quenched by the addition of 2× SDS buffer. Phosphorylated products were separated by 15% SDS-PAGE and analyzed on a PhosphorImager. Reaction samples performed with the peptide substrate were spotted onto Whatman P81 phosphocellulose paper, washed five times in 0.5% phosphoric acid, and dried. Incorporation of $^{32}$P was then quantified by Cerenkov counting.

Kinetic experiments were performed under the same conditions, except that the reaction was performed for 1 min. Reaction samples were spotted onto Whatman P81 phosphocellulose paper. Four different concentrations of histone H1 (2, 3, 5, and 10 μM) were used in the kinetic analysis of enzyme inhibition. For each substrate concentration, three concentrations of C4 peptide (0, 1, and 1.5 μM) were used, and the concentration of ATP was maintained constant at 0.1 mM. Similarly, when the concentration of ATP was varied (5, 10, 20, 30, 50, and 100 μM), C4 peptide concentrations were 0, 0.5, and 1 μM, and the concentration of histone H1 was kept constant at 15 μM. Using the Graphit Erithacus software, analysis of kinetic data for the inhibition of CDK2-cyclin A phosphorylation was performed by fitting the data to Equations 1 (non-competitive inhibition) and 2 (competitive inhibition),

$$v = (V_{max} \cdot [S]/(1 + [peptide]/K_i))/(K_m + [S]) \quad \text{(Eq. 1)}$$

$$v = V_{max} \cdot [S]/(K_m(1 + [peptide]/K_i) + [S]) \quad \text{(Eq. 2)}$$

where $V_{max}$ is the maximum velocity, [S] is the concentration of the varied substrate (ATP or histone H1), and $K_i$ is the dissociation constant for the CDK2-cyclin A-peptide complex.

*Peptide-CDK Binding Assays*—8 μg of preformed GST-CDK2-cyclin A or CDK2-GST-cyclin A complexes were incubated in buffer A with increasing concentrations of C4 or C6 peptides (corresponding to ~20, 40, and 90-fold the concentration of complex) at 25 °C for 30 min. GST complexes were then pulled down with glutathione-Sepharose beads and washed and eluted with buffer A containing 20 mM glutathione. Both the flow-through and the elution were analyzed by SDS-PAGE and Western blotting using antibodies against CDK2 (affinity-purified PSTAIRE polyclonal antibody) and cyclin A (H-432; Santa Cruz Biotechnology, Santa Cruz, CA).

*CD Experiments*—Far UV CD spectra were recorded on a JASCO J-810 spectropolarimeter (JASCO Corporation, Tokyo, Japan) using a quartz cuvette with a path length of 1 mm. Spectra were corrected from the baseline buffer spectrum and smoothed with JASCO software. Peptides were dissolved to a fixed concentration of 50 μM in water or phosphate-buffered solution. CD spectra were collected at 23 °C, and each spectrum represents the average of four scans.

*Cell Culture and Growth Inhibition Assays*—MCF-7, HepG2, and MDA-MB-231 cell lines were cultured at 37 °C and 5% $CO_2$ in Dulbecco's modified Eagle's medium containing 10% fetal bovine serum (Invitrogen). The human Jurkat lymphoma T cell line was cultured in RPMI 1640 complete medium. Cells were seeded at $2 \times 10^4$ cells/well in 24-well dishes and incubated overnight at 37 °C. Cells were then treated with increasing concentrations of peptides in 300 μl of OptiMEM for adherent cells and RPMI for Jurkat cells. After 45 min, 300 μl of medium containing 20% serum was added. After 48 h, cells were counted on a Coulter counter. The total number of cells was calculated as the percentage of treated to untreated cells. Concentrations of peptides indicated in each experiment correspond to those added in the 300 μl of OptiMEM during the first 45 min of treatment.

*Surface Plasmon Resonance Experiments*—All experiments were performed at 25 °C using a Biacore 3000 (Biacore AB). CDK2, cyclin A, and complexes were immobilized on a carboxymethyl dextran sensor chip by *N*-hydrosuccinimide/1-ethyl-3-(3′-dimethylaminopropyl)carbodiimide hydrochloride (NHS/EDC) coupling as described by the manufacturer. Peptide samples were prepared at different concentrations in the range of 50 to 1000 nM in 50 mM Tris HCl (pH 8.0) buffer containing 150 mM NaCl, 2 mM EDTA, and 50 mM KCl and were injected (30 μl) over the sensor surface at a flow rate of 10 $\mu l \cdot s^{-1}$. After completion of the injection phase, dissociation was performed for 200 s at the same flow rate. The apparent association and dissociation rate constants were calculated using BIA Evaluation version 3.0, and binding curves were fitted using a simple 1:1 Langmuir two-state reaction model.

*Molecular Graphics Representation of the Crystal Structure*—Coordinates of crystal structures used were downloaded from the Brookhaven Protein Data Bank (PDB code 1QMZ) (20, 23). The modeling package Discover/Insight II (MSI Inc.; San Diego, CA) and DeLano Scientific LLC PyMol software version 0.93 (DeLano Scientific, San Carlos CA) were used to analyze the structure of CDK2-cyclin A.

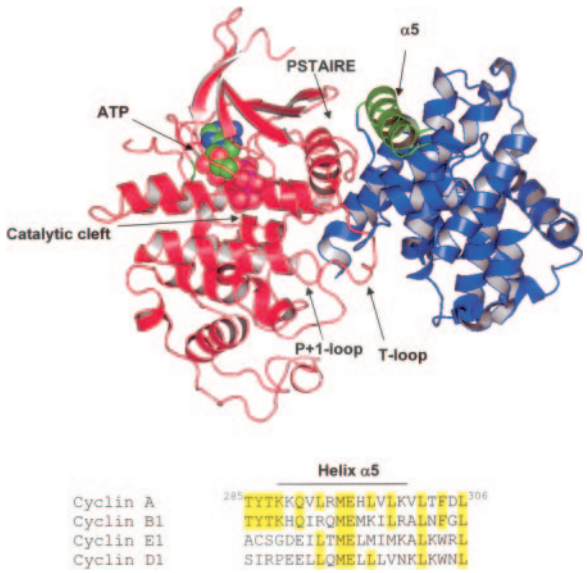


FIG. 1. **Ribbon diagram of CDK2-cyclin A structure and location of the interface domain.** At the *top* is a ribbon diagram of the structure of CDK2-cyclin A. CDK2 and cyclin A are depicted in *red* and *blue*, respectively. The cyclin A α5 helix is shown in *green*. Coordinates of crystal structures used were extracted from the Brookhaven Protein Data Bank (PDB code 1QMZ). The figure was generated using PyMol software version 0.93 (DeLano Scientific). Sequence alignments of the α5 helix of different cyclins (residues 285–306) are shown at the *bottom*. Sequence homologies are highlighted in *yellow*.

## RESULTS

*Design of Peptides Targeting Activation of CDK2-cyclin A*—Both the determination of the crystallographic structure of several CDKs and CDK-cyclin complexes in their inactive and active conformation and the characterization of their dynamics of association and activation have enabled identification of the critical features for activation of these complexes. The crystal structures of free CDK2 (24), cyclin A (17), and the unphosphorylated (16) and phosphorylated (25) CDK2-cyclin A complexes, respectively, have revealed that the regulatory cyclin subunit binds to one side of the catalytic cleft, interacting with both the N- and the C-lobes of the CDK to form a large, continuous protein-protein interface (Fig. 1). In addition, we have recently demonstrated that CDK2-cyclin A complex formation and activation is a two-step process (18). The first step involves the rapid association between the PSTAIRE helix of CDK2 and helices α3 and α5 of cyclin A, followed by a slow conformational change of the complex involving interactions between the N-terminal helix of cyclin A and the C-lobe of CDK2.

Based on these structural and biochemical characterizations, we propose a novel approach to specifically inhibiting the kinase activity of CDK-cyclin complexes by targeting protein-protein interfaces or conformational changes involved in their activation. To this aim, we have designed a peptide of 22 residues (C1) corresponding to the sequence of the α5 helix of cyclin A encompassing residues $Thr^{285}$ to $Leu^{306}$ (Table I). Although contacts between PSTAIRE and the α5 helix of cyclin A are common to all CDK-cyclin complexes (26), the primary sequence of C1 is only partially conserved between different cyclins (Fig. 1).

We first investigated the ability of C1 peptide to inhibit CDK2-cyclin A kinase activity. Three different substrates were used: (i) histone H1, which is most commonly used in standard kinase assays; (ii) a GST-fusion of the retinoblastoma protein (GST-Rb); and (iii) a peptide of 10 residues (PKTPKKAKKL) derived from histone H1 and reported to be a relevant substrate for measuring CDK1 or CDK2 kinase activity (27). As shown in Fig. 2, *A* and *B*, we found that C1 peptide significantly inhibits phosphorylation of all three of the above-mentioned substrates by CDK2-cyclin A *in vitro* in a dose-dependent manner. $IC_{50}$ values of 3.9 ± 0.4, 22.8 ± 1.2, and 2.2 ± 0.1 μM were calculated for histone H1, GST-Rb, and the peptide substrate, respectively.

*Identification of Critical Residues for Inhibitory Activity of the C1 Peptide*—To determine which residues were critical for inhibition of CDK2-cyclin A kinase activity by the C1 peptide, we replaced several individual residues with alanine and deleted residues reported to be involved in the contacts between CDK2 and the α5 helix of cyclin A. The ability of the different peptides (C1–C9) to affect the phosphorylation of histone H1 by CDK2-cyclin A is reported in Table I. Noteworthily, the peptide corresponding to part of C1 extended at its N terminus (C7) does not exhibit any inhibitory activity. Similarly, the addition of amino acids to the C-terminal $Leu^{306}$ decreases the inhibitory potential of the peptide (C8), suggesting that the integrity of C1 is required for robust inhibition. However, the three first N-terminal residues of the C1 peptide are not essential (C9), in contrast to residues 293 to 296, which appear to play a key role in the functional integrity of C1 (except for $Glu^{295}$ which is conserved between cyclins A, B, and E) (Fig. 1). Moreover, the greatest inhibition of kinase activity is obtained when $Glu^{295}$ is mutated to an alanine (C4), a mutation that increases the solubility of the peptide. Additional residues, which are not directly involved in the interface with CDK2, are also required for inhibition, such as $Leu^{299}$ (C6) and $Met^{294}$ (C3). Taken together, these results suggest that the region in the peptide that contributes primarily to kinase inhibition is located between residues 293 and 306.

Given that C4 exhibited the greatest potential to inhibit CDK2-cyclin A activity, it was chosen as the main focus for the rest of the study. The C4 peptide prevents phosphorylation of histone H1, GST-Rb, and the small peptide substrate derived from histone H1 by CDK2-cyclin A with estimated $IC_{50}$ values of 1.8 ± 0.1, 16.7 ± 0.6, and 1.1 ± 0.3 μM, respectively.

To evaluate the selectivity of the C4 peptide for the CDK2 isoform, we tested its ability to inhibit other CDK complexes, including CDK2-cyclin E and CDK1-cyclin B. The C4 peptide inhibits the kinase activity of CDK2 associated with either cyclin A ($IC_{50}$ of 1.8 ± 0.1 μM) or cyclin E ($IC_{50}$ of 1.5 ± 0.3 μM) to a similar extent, but it does not significantly affect CDK1-cyclin B kinase activity ($IC_{50}$ > 200 μM). In addition, C4 was not found to inhibit protein kinase A or protein kinase C (data not shown), suggesting that this peptide is specific to the CDK-cyclin complex and does not affect other protein kinases.

*Structural Characterization of the Inhibitory Peptides by Circular Dichroism*—To determine whether the inhibitory potential of the different peptides was associated with structural constraints, we examined their secondary structure by circular dichroism. Peptides are not folded in water solution. Each peptide was dissolved in the same phosphate buffer used for kinase activity assays at a final concentration of 50 μM. Peptides were divided into three classes based on their secondary structures as follows: (i) peptides C3, C6, C7, and C8, which are predominantly random coiled (Fig. 3*A*); (ii) peptides C2 and C9, which aggregate into β-structure, characterized by a positive contribution at 198 nm and a large negative band near 220 nm (Fig. 3*B*); and (iii) C4, which tends to adopt an α-helical structure characterized by two minima at 208 and 222 nm, respectively. The spectrum of C5 peptide is suggestive of a mixture of different structures.

The crystal structure of CDK2-cyclin A indicates that interactions between the α5-helix of cyclin A and the N-terminal

TABLE I
*Design and characterization of peptides derived from cyclin A*

The sequence of cyclin A α5 helix and the peptide directly derived from this helix (C1) together with its alanine scan mutants and other peptides used in this study are listed. Residues encompassed in the α5 helix of cyclin A are highlighted in gray, and mutations are in bold. $IC_{50}$ values for inhibition of CDK2 by the different peptides were estimated from dose-response kinase assays using histone H1 as a substrate. Each experiment was performed independently three times and expressed as mean ± S.E.

| Peptides | | $IC_{50}$ (μM) |
|---|---|---|
| cyclin A | $^{275}$VAEFVYITDDTYTKKQVLRMEHLVLKVLTFDLAAPTINQF$^{314}$ | |
| C1 | $^{285}$TYTKKQVLRMEHLVLKVLTFDL$^{306}$ | 3.9 ± 0.4 |
| C2 | TYTKKQVL**A**MEHLVLKVLTFDL | no inhibition |
| C3 | TYTKKQVLR**A**EHLVLKVLTFDL | > 50 |
| C4 | TYTKKQVLRM**A**HLVLKVLTFDL | 1.8 ± 0.1 |
| C5 | TYTKKQVLRME**A**LVLKVLTFDL | > 50 |
| C6 | TYTKKQVLRMEHLV**A**KVLTFDL | no inhibition |
| C9 | KKQVLRM**A**HLVLKVLTFDL | 11.1 ± 0.9 |
| C7 | YPPEVAEFVYITDDTYTKKQVL | no inhibition |
| C8 | RMEHLVLKVLTFDLAAPTVNQF | 28.4 ± 1.2 |
| C4-Tat | TYTKKQVLRM**A**HLVLKVLTFDLCRRRQRRKKRG | 2.2 ± 0.1 |

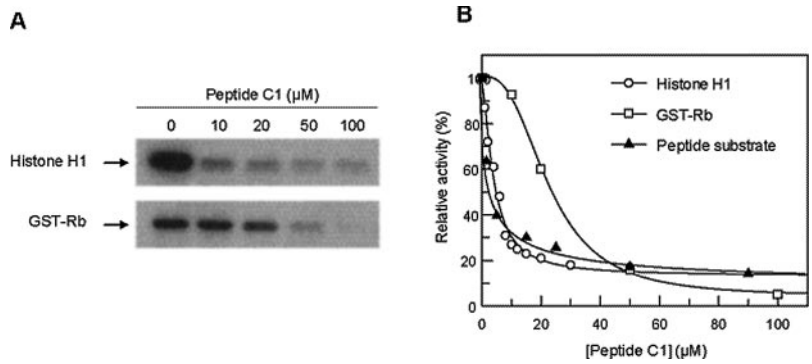


FIG. 2. **Inhibition of CDK2-cyclin A kinase activity by the C1 peptide.** *A*, increasing concentrations of the C1 peptide (0–100 μM) were mixed with CDK2-cyclin A prior to the addition of either histone H1 or GST-Rb substrates. *In vitro* kinase reactions were performed as described under "Experimental Procedures," and the phosphorylation levels of substrates were quantified by autoradiography. *B*, relative inhibition of substrate phosphorylation (histone H1, GST-Rb, and the small histone H1-derived peptide) by C1 peptide.

β-sheet of CDK2 are essentially hydrophobic. Thus the α-helical structure of C4 peptide, which is stabilized in the presence of salt, may favor hydrophobic interactions with CDK2-cyclin A associated with its inhibitory potential.

*Mechanism of Inhibition of CDK2 Activity by the C4 Peptide*—C4-mediated inhibition of CDK2 can result from either direct competition with cyclin A for CDK2 or from the binding of the peptide to the preformed CDK2-cyclin A complex. To discriminate between these two hypotheses, we performed direct competition experiments in which various concentrations of peptide (inhibiting kinase activity by 90%) were added to a mixture of either GST-CDK2 and cyclin A or GST-cyclin A and CDK2 (Fig. 4). The different CDK2-cyclin A complexes were isolated with glutathione-Sepharose beads. Levels of cyclin A associated with GST-CDK2 or CDK2 bound to GST-cyclin A were determined by Western blotting, and kinase activity of these complexes toward histone H1 was evaluated. As shown in Fig. 4, the addition of C4 strongly inhibits kinase activity of CDK2 without inducing dissociation of cyclin A from CDK2, irrespective of the method used. Moreover, similar kinase inhibition was obtained by adding the peptide either before or after reconstitution of the CDK2-cyclin A complex (data not shown). Based on these experiments, we infer that the C4 peptide maintains CDK2-cyclin A in an inactive or non-processive conformation but does not disrupt the complex.

To gain further insight into the mechanism that governs binding of the C4 peptide to CDK2-cyclin A, we studied the kinetics of binding using surface plasmon resonance (Fig. 5*A*). Binding curves were recorded by injecting increasing concentrations of C4 onto a flow cell on which either CDK2, cyclin A, or CDK2-cyclin A had been cross-linked. As shown in Fig. 5*B*, C4 interacts tightly with CDK2-cyclin A with an estimated dissociation constant of 2.5 ± 0.4 nM and with an 18-fold lower affinity for cyclin A ($K_d$ = 45 ± 2 nM). In contrast, C4 does not bind monomeric CDK2. These results support the idea that C4 forms a ternary complex with CDK2-cyclin A.

*Steady-state Analysis of CDK2 Inhibition by the C4 Peptide*—We next investigated the steady-state kinetics of inhibition of CDK2-cyclin A by C4 using Michaelis-Menten equations. Phosphorylation of histone H1 by CDK2-cyclin A was measured in the presence of increasing concentrations of ATP and in the absence or presence of the C4 peptide. In this experiment, the concentration of the H1 substrate was fixed at 15 μM, which represents approximately three times the $K_m$ of CDK2-cyclin A for histone H1 ($K_{m_{(H1)}}$ = 3.4 μM). The double reciprocal Lineweaver-Burk plot reveals that C4 acts as a non-competitive inhibitor with respect to ATP (Fig. 6*A*). The dissociation constant ($K_i$) of the C4 peptide from the free enzyme is 0.34 ± 0.04 μM. We next examined inhibition by C4 with respect to histone H1 substrate in the presence of a saturating concentration of ATP (0.1 mM ATP, $K_{m_{(ATP)}}$ = 32 μM). The pattern of the double reciprocal plot for histone H1 is consistent with a competitive mode of inhibition with a value of $K_i$ of 0.35 ± 0.04 μM.

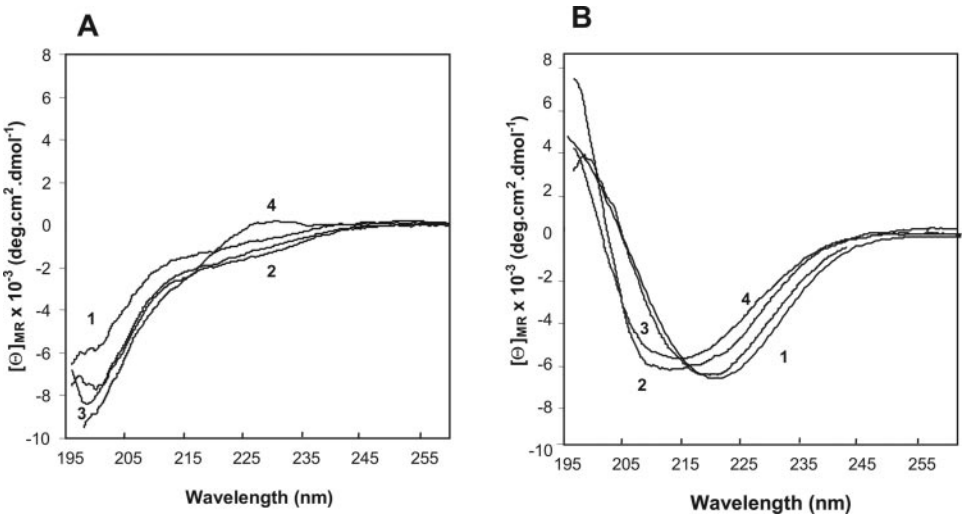


FIG. 3. **CD spectra of the different peptides.** Experiments were performed at 23 °C using a concentration of peptides of 50 $\mu$M in phosphate-buffered saline. *A*, CD spectra of peptides C6 (*trace 1*), C8 (*trace 2*), C3 (*trace 3*), and C7 (*trace 4*) are characteristic of a random coiled state. *B*, CD spectra of C2 (*trace 3*) and C9 (*trace 1*) exhibit a large negative band near 220 nm that is characteristic of $\beta$-sheet aggregates. The spectrum of C4 (*trace 2*) is characterized by two minima at 208 and 222 nm, indicative of a predominantly $\alpha$-helical structure. The spectrum of C5 (*trace 4*) is suggestive of a mixture of different structures.

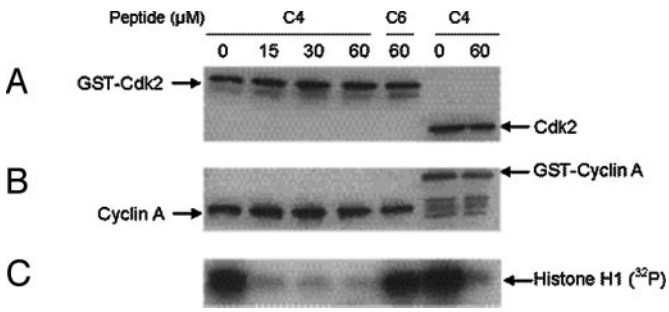


FIG. 4. **Effect of C4 peptide on formation of CDK2-cyclin A complex.** *A* and *B*, increasing concentrations of C4 and C6 peptides were added to GST-CDK2-cyclin A (*lanes 1* to *5*, from the *left*) or GST-cyclin A-CDK2 (*lanes 6* and *7*). GST-tagged proteins were then precipitated using glutathione-Sepharose beads. Levels of GST-CDK2 or CDK2 (*A*) and GST-cyclin A or cyclin A (*B*) were determined by Western blotting using anti-PSTAIRE or anti-cyclin A antibodies, respectively. *C*, residual kinase activities were evaluated as the level of histone H1 phosphorylation revealed by autoradiography.

The C4 peptide binds the active site of CDK2 to interfere with the interaction of the substrate independently of ATP binding in the catalytic site. The ability of C4 to inhibit phosphorylation of the small histone H1-derived peptide (PKTPKKAKKL) suggests that C4 binds close to the interface between CDK2 and cyclin A. We have docked this peptide substrate of 10 residues into the x-ray structure of the CDK2-cyclin A-peptide complex reported by Brown *et al.* (23), and we find that the substrate-binding site overlaps with both subunits. The residues AKKL at the C terminus of the peptide substrate form close contacts with residues in the $\alpha$3 helix (Ala$^{264}$ and Phe$^{267}$) and the loop connecting the $\alpha$3 and $\alpha$4 helices (Ile$^{270}$ and Tyr$^{271}$) of cyclin A (Fig. 7).

*C4 Peptide Inhibits Human Cancer Cell Proliferation*—We finally investigated whether C4 affected proliferation of human cancer cell lines. Exponentially growing cultures of the estrogen-independent MDA-MB-231 breast cancer cell line were cultured in the absence or presence of various concentrations of the C4, C6, or C7 peptides (Fig. 8). The C4 peptide induced a slightly inhibited proliferation of these cells in a dose-dependent manner ($IC_{50}$ of ~25 $\mu$M), whereas the C6 and C7 peptides had no effect after 48 h of treatment, which is consistent with the *in vitro* kinase assays. We attributed the 20-fold lower efficiency of C4 in cell culture in comparison to its *in vitro* kinase inhibition to inefficient cellular uptake of the peptide. To increase the cellular uptake of C4, we therefore covalently linked it to the protein transduction domain derived from the human immunodeficiency virus Tat protein through a disulfide bond (28). The conjugation of C4 to the carrier peptide Tat did not affect its *in vitro* inhibitory activity ($IC_{50}$ = 2.2 ± 0.1 $\mu$M) but significantly improved its efficiency on cultured cells. MDA-MB-231 cells were incubated in the presence of various concentrations of C4-Tat, C4, and Tat ranging from 5 to 30 $\mu$M, and cell proliferation was examined after 48 h. As shown in Fig. 8, C4-Tat inhibits cell proliferation in a dose-dependent manner with an $IC_{50}$ 3-fold greater than that of free peptide (7.5 ± 0.3 $\mu$M). As a control, we verified that the Tat peptide did not affect cell growth in the range of concentrations used. We evaluated the effect of C4-Tat peptide on several human tumor cell lines and found that proliferation of all the cell lines was affected by C4-Tat in the low micromolar range. $IC_{50}$ values of 2.0 ± 0.6, 11.9 ± 0.1, and 14.2 ± 0.3 $\mu$M were obtained for Jurkat, MCF-7, and HepG2 cell lines, respectively (Table II).

## DISCUSSION

Protein kinases constitute important targets in cancer chemotherapy (4). In the last few years, several CDK inhibitors, essentially ATP antagonists, have been developed and assayed at the preclinical and clinical level (6). One of the major drawbacks of inhibitors that target the ATP-binding site of the kinase is their poor selectivity for a single CDK isoform. In the present work we propose a new strategy for the design of selective CDK inhibitors that involves targeting interface domains or the conformational changes required for activation of CDK protein kinases. Although the relevance of the targets and the specificity of the cell cycle regulators remain issues (29), the design of CDK inhibitors with unique selectivity offers the potential to treat a wide range of tumor types.

As both the structure and the mechanism of CDK2-cyclin A have been extensively characterized, we chose to target this complex as a proof of principle. Crystal structures of cyclin A in its free (17) and CDK2-bound state (16) reveal that the cyclin box (residues 209–310) constitutes the main interface with CDK2 through interactions with the PSTAIRE helix and contacts with the T-loop as well as with the N-terminal $\beta$-sheet of

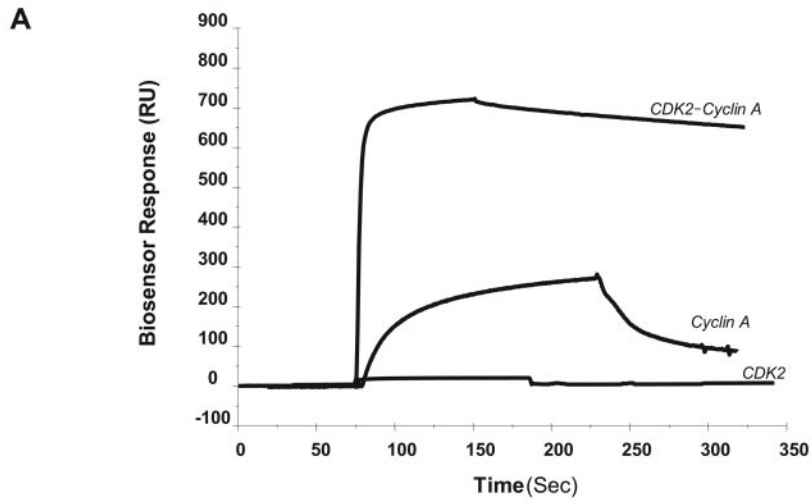


FIG. 5. **Binding of C4 peptide to CDK2-cyclin A, cyclin A, and CDK2 by surface plasmon resonance.** *A*, increasing concentrations of C4 peptide were injected over CDK2, cyclin A, or CDK2-cyclinA immobilized on the chips. The association and dissociation phase data for a subset of C4 peptide concentrations were fitted using a simple 1:1 Langmuir model using Biacore evaluation software. *B*, rate constants and $K_d$ values derived from surface plasmon resonance data analysis for C4 peptide binding to the CDK2-cyclin A complex and to cyclin A.

B

| Interaction | $k_{on}$ ($M^{-1}.s^{-1}$) | $k_{off}$ ($s^{-1}$) | *Kd* (nM) |
|---|---|---|---|
| Peptide C4 + CDK2-Cyclin A | $2.1 \times 10^5$ | $5.2 \times 10^{-4}$ | 2.5 ± 0.4 |
| Peptide C4 + Cyclin A | $7.4 \times 10^4$ | $3.3 \times 10^{-3}$ | 45 ± 2 |

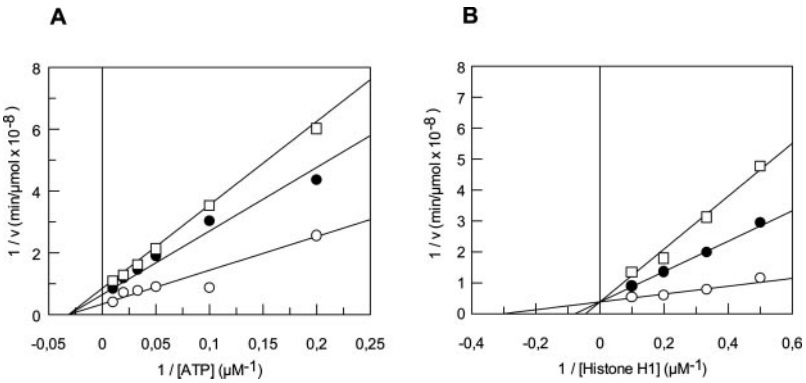


FIG. 6. **Mechanism of inhibition of CDK2-cyclin A by the C4 peptide.** CDK2-cyclin A activity was monitored as described under "Experimental Procedures," and data were fitted according to a double reciprocal plot. *A*, inhibition of CDK2-cyclin A activity by C4 as a function of ATP. Experiments were performed with a fixed 15 µM concentration of histone H1 in the absence (*empty circle*) or presence of 0.5 µM (*filled circle*) and 1 µM (*square*) peptide C4. *B*, inhibition of CDK2-cyclin A activity by C4 as a function of histone H1. Experiments were performed with a fixed 0.1 mM concentration of ATP in the absence (*empty circle*) or presence of 0.5 µM (*filled circle*) and 1 µM (*square*) C4.

CDK2. The major contacts involve the α3, α4, and α5 helices of cyclin A, which are critical for the first step of complex formation (18). With the aim of specifically targeting the protein-protein interface between CDK2 and cyclin A, we therefore designed and characterized a series of peptides derived from the α5 helix of cyclin A.

We have identified a peptide of 22 residues (C4) which, in contrast to the majority of the CDK-cyclin ATP antagonist inhibitors described so far, neither competes with ATP nor affects activity of other protein kinases. C4 peptide is highly specific for complexes harboring CDK2 and inhibits its kinase activity at low concentrations ($K_i$ = 340 nM) in a competitive fashion with respect to the phosphoacceptor substrate. We have shown that C4 peptide adopts an α-helical structure, which is consistent with the idea that the conformational constraint imposed by an α-helix allows key contacts between C4 and the CDK2-cyclin A complex.

Several competitive peptide inhibitors of CDKs have been described previously (11). A large majority are based on the CBM, a consensus sequence common to a number of substrates and inhibitors of mammalian CDKs. The CBM sequence is essential for substrate recognition and interacts with a hydrophobic patch on the surface of cyclin A (30, 31). This docking site on cyclin A is known to be critical for the phosphorylation of substrates containing the CBM, such as Rb, but unlike histone H1. Inhibitory peptides derived from the C terminus of

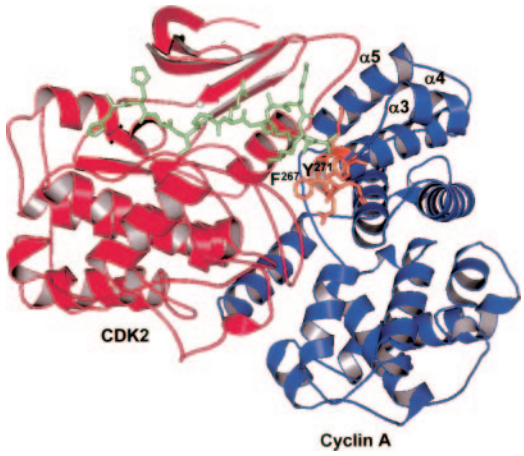


FIG. 7. **Contacts between CDK2-cyclin A and the substrate peptide.** Ribbon diagram of the structure of the CDK2-cyclin A-peptide. CDK2, cyclin A, and the peptide are depicted in *red*, *blue*, and *green*, respectively. The 10-residue peptide substrate was docked onto the structure of CDK2-cyclin A using the structure of the CDK2-cyclinA-substrate peptide reported by Brown *et al.* (23). Coordinates of crystal structures used were extracted from the Brookhaven Protein Data Bank (PDB code 1QMZ). The side chain of key residues in the α3 helix and the loop connecting the α3 and α4 helix are shown in *orange*. The figure was generated using PyMol software version 0.93 (DeLano Scientific). $F^{267}$, $Phe^{267}$; $Y^{271}$, $Tyr^{271}$.

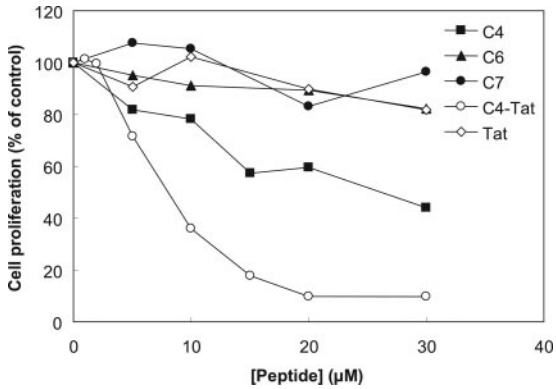


FIG. 8. **Anti-proliferative effect of the C4 peptide on human cancer cells.** Exponentially growing human breast cancer cells (MDA-MB-231) were incubated in the presence of increasing concentrations of C4 (*closed square*), C6 (*closed triangle*), C7 (*closed circle*) and C4-Tat (*open circle*) in the absence of serum for 45 min, after which the concentration of serum was adjusted to 10%. Cells were treated in the same fashion with Tat (*open square*) as a control. After 48 h, the number of cells was counted with a Coulter counter. Each experiment was performed independently three times and expressed as mean ± S.E.

TABLE II
*Inhibition of tumor cell proliferation by C4-Tat peptide*

Cells were incubated with increasing concentrations of C4-Tat for 48 h. The number of cells was counted with a Coulter counter. Each experiment was performed independently three times and expressed as mean ± SE.

| Cell lines | $IC_{50}$ |
|---|---|
| | $\mu M$ |
| Jurkat | 2.0 ± 0.6 |
| MDA-MB-231 | 7.5 ± 0.3 |
| MCF-7 | 11.9 ± 0.1 |
| HepG2 | 14.2 ± 0.3 |

the CDK inhibitor $p21^{WAF1}$ or the transcription factor E2F1 compete directly with Rb for binding to the hydrophobic patch on the cyclin and, therefore, inhibit phosphorylation of other substrates like histone H1 quite poorly. On the other hand, peptide aptamers isolated from a combinatorial library behave as competitive inhibitors of CDK2 with respect to histone H1 but do not interfere with the phosphorylation of substrates interacting with the recruitment binding site on cyclin A, such as Rb (32). In contrast to these two families of peptide inhibitors, the C4 peptide blocks phosphorylation of both histone H1 and Rb. This being said, C4-mediated inhibition is 10-fold greater for histone H1 ($IC_{50}$ = 1.8 ± 0.1 $\mu$M) than for Rb ($IC_{50}$ = 16.7 ± 0.6 $\mu$M), suggesting that C4 does not interact with the hydrophobic pocket of cyclin A. Moreover, given that C4 peptide competitively inhibits the phosphorylation of the small histone H1-derived peptide, it is likely that its binding site overlaps with the substrate-binding site.

We have demonstrated that the C4 peptide does not compete with cyclin A for the interaction with CDK2 but instead forms stable complexes with CDK2-cyclin A. Brown *et al.* (23) have reported that the short substrate peptide (HHASPRK) binds the catalytic site essentially through contacts with the C-terminal lobe of CDK2. By docking longer peptides onto the structure of CDK2-cyclin A, we have shown that residues in $\alpha$3 and in the loop connecting the $\alpha$3 and $\alpha$4 helices of cyclin A make close contacts with the peptide substrate and should therefore be considered as part of the substrate-binding site. Taking these results together with the finding that C4 associates with cyclin A but not with monomeric CDK2, we suggest that the binding of cyclin induces a conformational change in CDK2 that exposes the docking site on the CDK, thereby facilitating binding of the C4 peptide across the catalytic cleft of CDK2. We believe that the P + 1 loop of CDKs that is involved in organizing the catalytic site of these kinases, being stabilized upon the binding of cyclin, is a good candidate interaction site for C4 (26). A growing number of studies suggest that the protein kinase docking sites that mediate substrate phosphorylation may represent effective targets for inhibitor design. Recently, peptides derived from a high affinity site on CDK2 required for p53 phosphorylation were shown to successfully inhibit p53 phosphorylation in a melanoma cell line (33). Peptides based on the c-Jun N-terminal kinase (JNK)-binding domain (JIP1) of JNK I were shown to inhibit JNK activity both *in vitro* and *in vivo* when associated with a cell-penetrating peptide (34, 35).

In conclusion, we have described a new class of small peptide inhibitors of cell cycle progression that target essential conformational changes involved in CDK2-cyclin A activation. In contrast to most kinase inhibitors described in the last few years, the prototype peptide of this study (C4) neither competes with ATP nor binds the hydrophobic patch of cyclin A. We have validated the efficacy of this peptide strategy *in cellulo* by demonstrating that tumor cell proliferation is blocked in a dose-dependent fashion when the C4 peptide is coupled to the cell-penetrating carrier Tat. Additional studies are in progress to characterize the mechanism of action and to identify the precise binding site of the C4 peptide on CDK2-cyclin A.

*Acknowledgments*—We are grateful to F. Heitz for critical reading of the manuscript and helpful discussions. We thank J. Endicott, D. Morgan, S. Reed, and C. Sardet for plasmids and proteins used in this work and E. Vives for Tat conjugation expertise.

REFERENCES

1. Morgan, D. O. (1997) *Annu. Rev. Cell Dev. Biol.* **13,** 261–291
2. Malumbres, M. & Carnero, A. (2003) *Prog. Cell Cycle Res.* **5,** 5–18
3. Gali-Muhtasib, H. & Bakkar, N. (2002) *Curr. Cancer Drug Targets* **2,** 309–336
4. Dancey, J. & Sausville, E. A. (2003) *Nat. Rev. Drug Discov.* **2,** 296–313
5. Noble, M. E. M., Endicott, J. & Johnson, L. N. (2004) *Science* **303,** 1800–1805
6. Swanton, C. (2004) *Lancet Oncol.* **5,** 27–36
7. Huwe, A., Mazitschek, R. & Giannis, A. (2003) *Angew. Chem. Int. Ed. Engl.* **42,** 2122–2138
8. Bain, J., McLauchlan, H., Elliott, M. & Cohen, P. (2003) *Biochem. J.* **371,** 199–204
9. Fischer, P. M., Endicott, J. & Meijer, L. (2003) *Prog. Cell Cycle. Res.* **5,** 235–248
10. Serendowicz, A. M. (2003) *Oncogene* **22,** 6606–6620
11. McInnes, C., Andrews, M. J. I., Zheleva, D. I., Lane, D. P. & Fischer, P. M. (2003) *Curr. Med. Chem. Anti-Cancer Agents* **3,** 57–69
12. Ball, K. L., Lain, S., Fåhraeus, R., Smythe, C. & Lane, D. P. (1996) *Curr. Biol.* **7,** 71–80
13. Chen, Y. N. P., Sharma, S. K., Ramsey, T. M., Jiang, L., Martin, M. S., Baker, K., Adams, P. D., Bair, K. W. & Kaelin, W. G. (1999) *Proc. Natl. Acad. Sci. U. S. A.* **96,** 4325–4329
14. Mendoza, N., Fong, S., Marsters, J., Koeppen, H., Schwall, R. & Wickramasinghe, D. (2003) *Cancer Res.* **63,** 1020–1024
15. Pavletich, N. P. (1999) *J. Mol. Biol.* **287,** 821–828
16. Jeffrey, P. D., Russo, A. A., Polyak, K., Gibbs, E., Hurwitz, J., Massagué, J. & Pavletich, N. P. (1995) *Nature* **376,** 313–320
17. Brown, N. R., Noble, M. E. M., Endicott, J. A., Garman, E. F., Wakatsuki, S., Mitchell, E., Rasmussen, B., Hunt, T. & Johnson, L. N. (1995) *Structure*, **3,** 1235–1247
18. Morris, C. M., Gondeau, C., Tainer, J. A. & Divita, G. (2002) *J. Biol. Chem.* **277,** 23847–23853
19. Heitz, F., Morris, M. C., Fesquet, D., Cavadore, J. C., Doree, M. & Divita, G. (1997) *Biochemistry* **36,** 4995–5003
20. Brown, N. R., Noble, M. E., Lawrie, A. M., Morris, M. C., Tunnah, P., Divita, G., Johnson, L. N. & Endicott, J. A. (1999) *J. Biol. Chem.* **274,** 8746–8756
21. Desai, D., Wessling, H. C., Fisher, R. P. & Morgan, D. O. (1995) *Mol. Cell. Biol.* **15,** 345–350
22. Spruck, C., Strohmaier, H., Watson, M., Smith, A. P., Ryan, A., Krek, T. W. & Reed, S. I. (2001) *Mol. Cell.* **7,** 639–650
23. Brown, N. R., Noble, M. E., Endicott, J. A. & Johnson, L. N. (1999) *Nat. Cell Biol.* **1,** 438–443
24. De Bondt, H. L., Rosenblatt, J., Jancarik, J., Jones, H. D., Morgan, D. O. & Kim, S. H. (1993) *Nature* **363,** 595–602
25. Russo, A. A., Jeffrey, P. D., Russo, A. A. & Pavletich, N. P. (1996) *Nat. Struct. Biol.* **3,** 696–700
26. Nolen, B., Taylor, S. & Ghosh, G. (2004) *Mol. Cell* **15,** 661–675
27. Beaudette, K. N., Lew, J. & Wang, J. H. (1993) *J. Biol. Chem.* **268,** 20825–20830
28. Wadia, J. S., Stan, R. V. & Dowdy, S. F. (2004) *Nat. Med.* **10,** 310–315

29. Fischer, P. M. (2004) *Cell Cycle* **6,** 742–746
30. Schulman, B. A., Lindstrom, D. L. & Harlow, E. (1998) *Proc. Natl. Acad. Sci. U. S. A.* **95,** 110453–110458
31. Lowe, E. D., Tews, I., Cheng, K. Y., Brown, N. R., Gul S., Noble M. E., Gamblin S. J. & Johnson, L. N. (2002) *Biochemistry* **41,** 15625–15634
32. Cohen, B. A., Colas, P. & Brent, R. (1998) *Proc. Natl. Acad. Sci. U. S. A.* **95,** 14272–14277
33. Ferguson, M., Luciani, M. G., Finlan, L., Rankin, E. M., Ibbotson, S., Fersht, A. & Hupp, T. R. (2004) *Cell Cycle* **3,** 80–89
34. Barr, R. K., Boehm, I., Attwood, P. V., Watt, P. M. & Bogoyevitch, M. A. J. (2004) *Biol. Chem.* **279,** 36327–36338
35. Kaneto, H., Nakatani, Y., Miyatsuka, T., Kawamori, D., Matsuoka, T. A., Matsuhisa, M., Kajimoto, Y., Ichijo, H., Yamasaki, Y. & Hori, M. (2004) *Nat. Med.* **10,** 1128–1132